An Anionic Phospholipid Enables the Hydrophobic Surfactant Proteins to Alter Spontaneous Curvature

Mariya Chavarha,[†] Ryan W. Loney,[†] Shankar B. Rananavare,[‡] and Stephen B. Hall[†*]

[†]Departments of Biochemistry and Molecular Biology, Medicine, and Physiology and Pharmacology, Oregon Health & Science University, Portland, Oregon; and [‡]Department of Chemistry, Portland State University, Portland, Oregon

ABSTRACT   The hydrophobic surfactant proteins, SP-B and SP-C, greatly accelerate the adsorption of the surfactant lipids to an air/water interface. Previous studies of factors that affect curvature suggest that vesicles may adsorb via a rate-limiting structure with prominent negative curvature, in which the hydrophilic face of the lipid leaflets is concave. To determine if SP-B and SP-C might promote adsorption by inducing negative curvature, we used small-angle x-ray scattering to test whether the physiological mixture of the two proteins affects the radius of cylindrical monolayers in the inverse hexagonal phase. With dioleoyl phosphatidylethanolamine alone, the proteins had no effect on the hexagonal lattice constant, suggesting that the proteins fail to insert into the cylindrical monolayers. The surfactant lipids also contain ~10% anionic phospholipids, which might allow incorporation of the cationic proteins. With 10% of the anionic dioleoyl phosphatidylglycerol added to dioleoyl phosphatidylethanolamine, the proteins induced a dose-related decrease in the hexagonal lattice constant. At 30°C, the reduction reached a maximum of 8% relative to the lipids alone at ~1% (w/w) protein. Variation of NaCl concentration tested whether the effect of the protein represented a strictly electrostatic effect that screening by electrolyte would eliminate. With concentrations up to 3 M NaCl, the dose-related change in the hexagonal lattice constant decreased but persisted. Measurements at different hydrations determined the location of the pivotal plane and proved that the change in the lattice constant produced by the proteins resulted from a shift in spontaneous curvature. These results provide the most direct evidence yet that the surfactant proteins can induce negative curvature in lipid leaflets. This finding supports the model in which the proteins promote adsorption by facilitating the formation of a negatively curved, rate-limiting structure.

INTRODUCTION

The first step that must occur for pulmonary surfactant to lower surface tension in the lungs is the formation of an interfacial film. Within seconds after a baby takes its initial breath and inflates the fluid-filled alveolus with air [1,2], the surfactant constituents adsorb to the air/liquid interface. Experiments in vitro show that constituents of surfactant vesicles adsorb collectively rather than individually [3–5], suggesting that vesicles fuse with the interface to deliver their components together. As in the case of the fusion of two bilayers [6], several exogenous compounds affect the rate of adsorption according to how they modify the curvature of phospholipid leaflets. Phosphatidylethanolamines (PEs) and gramicidin-A induce lipid leaflets to adopt curvature that is negative, with a concave hydrophilic face. These compounds promote faster adsorption [7–10]. Lysophosphatidylcholine, which contributes to positive curvature of a leaflet [11], inhibits adsorption [12]. These findings suggest that negative curvature represents an important characteristic of a kinetic intermediate that limits the rate of adsorption.

The hydrophobic surfactant proteins (SPs), SP-B and SP-C, greatly accelerate adsorption of the surfactant lipids [10,13]. The relationship between curvature and kinetics established for exogenous modulators suggests that the proteins may achieve their effect by promoting the formation of a negatively curved, rate-limiting structure. The proteins could reduce the energy required to bend the lipid leaflets into the curved configuration. Each leaflet has a spontaneous curvature (c_o) that it adopts in the absence of applied force. The proteins could shift the c_o toward the curvature of the intermediate, or they might reduce the bending elasticities that determine the energy required to bend the leaflets between two configurations [15]. The experiments reported here tested whether the proteins affect c_o.

Measurements of c_o require the cylindrical monolayers of the inverse hexagonal (H_{II}) phase. In lamellar bilayers, c_o for the individual leaflets remains unexpressed. The c_o for each monolayer cancels the curvature of the oppositely oriented, paired leaflet, resulting in a planar bilayer [16]. The PEs that form the H_{II} phase represent only a few percent of the phospholipids in pulmonary surfactant [17]. Our experiments therefore must use model lipids.

Any effect of the proteins on the curvature of a monolayer in the H_{II} phase should extend to the surfactant lipids. The effective molecular shape of lipids, established by the relative cross-sectional areas of the hydrophilic and hydrophobic ends of the molecule, in large part determines the polymorphic structures that they form [18–20]. Shape is a colligative property [16], and the c_o of a leaflet reflects the weighted average of the shape for its constituents [21,22]. Any change in c_o produced by the proteins and measured from a shift in the size of the hexagonal lattice should also occur in the bilayers formed by the surfactant lipids. The change in c_o would

be hidden in the lamellar bilayers at equilibrium, but essential for the transient formation of the hypothetical curved intermediate that limits the rate of adsorption (23).

The experiments reported here follow directly from a previous study (24), which showed that the hydrophobic SPs can promote curved structures. In amounts as low as 0.01% (w/w), the SPs induce 1-palmitoyl-2-oleoyl phosphatidylethanolamine (POPE) to convert from lamellar bilayers to the saddle-shaped network of the bicontinuous inverse cubic (Q_{II}) phases (24). The efficiency of the proteins, however, in producing these alterations prevents evaluation of whether they change c_o. The H_{II} phase, which provides the individual monolayers necessary to evaluate c_o, was largely absent from mixtures of the proteins with POPE. Above 0.03% SP, samples contained only the bilayers of the Q_{II} phases (24).

The studies reported here attempted to circumvent this problem by using a different lipid. Dioleoyl phosphatidylethanolamine (DOPE) forms H_{II} structures at lower temperatures than POPE. If, during heating, the most stable structures follow the sequence $L_\alpha \rightarrow Q_{II} \rightarrow H_{II}$ (25,26), then lipid-protein mixtures that initially form a Q_{II} phase might still convert to H_{II} structures at higher temperatures. DOPE, by forming H_{II} structures at lower temperatures than POPE, maximized the chances of observing the H_{II} phase with the proteins in the range of accessible temperatures. We combined DOPE with increasing amounts of the proteins and then heated the samples. We used small-angle x-ray scattering (SAXS) to establish the temperatures at which the H_{II} phase was present and to determine how the radius of the cylindrical monolayers responded to different amounts of the proteins.

MATERIALS AND METHODS

Materials

DOPE and dioleoyl phosphatidylglycerol (DOPG) were obtained from Avanti Polar Lipids (Alabaster, AL) and used without further purification or characterization. All solvents and reagents were ACS grade and used as received from the distributors: NaCl, CaCl₂, chloroform, and methanol from Mallinckrodt (Hazelwood, MO); UltraPure Na₂EDTA-2H₂O from Invitrogen (Grand Island, NY); NaN₃ from Teknova (Hollister, CA); and HEPES and HEPES Na salt from Acros Organics (Geel, Belgium). The combined hydrophobic proteins were separated from extracted calf surfactant, provided by Dr. Edmund Egan of ONY (Amherst, NY), by gel-permeation chromatography on a matrix of LH-20 using a solvent of chloroform:methanol (1:1, v/v) (27). The omission of the acid commonly included in the solvent (28) minimized the risk of cleavage (29) or covalent modifications (30). Water was processed and treated with ultraviolet light using a NANO-pure Diamond TOC-UV water-purification apparatus (Barnstead/Thermolyne, Dubuque, IA).

Methods

Biochemical determinations

Protein content was measured quantitatively by amido-black assay on material precipitated with trichloroacetic acid using bovine serum albumin as a standard (31). Phospholipid quantities were determined by measuring the amount of phosphate present (32).

Preparation of samples for x-ray diffraction

Samples with 0–5% SP were prepared from stock solutions of lipids in chloroform and proteins in chloroform/methanol (1:1, v/v). Solvent was initially evaporated from appropriate mixtures under a stream of nitrogen, followed by desiccation at 2 mbar overnight at room temperature. The resulting films were resuspended in the following aqueous media: 10 mM HEPES, pH 7.0, and 2 μM EDTA (HE) with varying salt concentrations (0–3 M NaCl); or 10 mM HEPES, pH 7.0, 150 mM NaCl, and 1.5 mM CaCl₂ (HSC). The antioxidant NaN₃ was present in all buffers at 0.002% (w/w). Films were hydrated overnight at 4°C and dispersed with cyclic freezing and thawing followed by vigorous vortexing. The samples were transferred to capillaries (special glass, diameter 1.0 mm, wall thickness 0.01 mm; Charles Supper, Natick, MA), which were centrifuged at $640 \times g_{max}$ for 10 min, sealed with flame and epoxy, and stored at 4°C.

Samples for analysis of the pivotal plane were prepared at specific hydrations. Appropriate volumes of lipid-protein solutions in chloroform were added to deliver ~4–8 mg phospholipid/capillary (boron-rich glass, diameter 2.0 mm, wall thickness 0.01 mm; Charles Supper). After preparation of dried samples as described above, appropriate weights of HE were added to achieve the desired hydration. Capillaries were then centrifuged at $640 \times g_{max}$ for 10 min before being sealed by flame. The final weight after sealing was used to determine the actual water content. The samples were temperature-cycled between −20°C and 4°C several times to promote sample mixing, and stored at 4°C. Calculated volume fractions (ϕ_w) obtained the molecular volume of water ($\overline{V}_w$) based on a density of 0.995 g/ml at 30°C. For the molecular volume of the lipid ($\overline{V}_\ell$), calculations assumed a value of 1.0 g/ml for both phospholipids.

Small-angle x-ray diffraction

Diffraction was measured on beamline 1–4 at the Stanford Synchrotron Radiation Lightsource (SSRL). Capillaries were mounted on an aluminum block, the temperature of which was controlled with water pumped from a circulating bath and monitored with an externally applied thermocouple. Block temperatures were converted to sample temperatures according to relationships established by monitoring the melting of a series of compounds with known melting points. Samples were equilibrated at each temperature for at least 10 min, after which they were exposed to an x-ray beam with a wavelength of 1.488 Å for 120 s. The diffracted intensities were radially integrated using the program Fit2D (33) to obtain plots of intensity versus the scattering vector (q). Spatial calibration was performed with standards of silver behenate, lead stearate, and cholesterol myristate. Lamellar, hexagonal, and cubic space groups were assigned according to the best fit of measured q-values for diffracted peaks to allowed Miller indices (24,34). The slopes of the lines provided the lattice constants (a_o) of the unit cells according to $a_o = 2\pi/\text{slope}$ for the lamellar and cubic phases, and $a_o = 4\pi/(\sqrt{3} \times \text{slope})$ for the hexagonal phase.

The results presented here were obtained from a single set of samples for each lipid mixture during a single visit to the SSRL. Additional measurements performed on three other sets of lipid-protein mixtures in EDTA and HSC during separate visits confirmed these results.

RESULTS

The proteins with DOPE

The SPs with DOPE demonstrated the same ability to induce formation of Q_{II} phases found previously with POPE. As expected from calorimetric studies (35), the lipid alone formed a hexagonal phase over the full range of accessible temperatures (Figs. 1 *A* and 2 *A*). With the lowest level
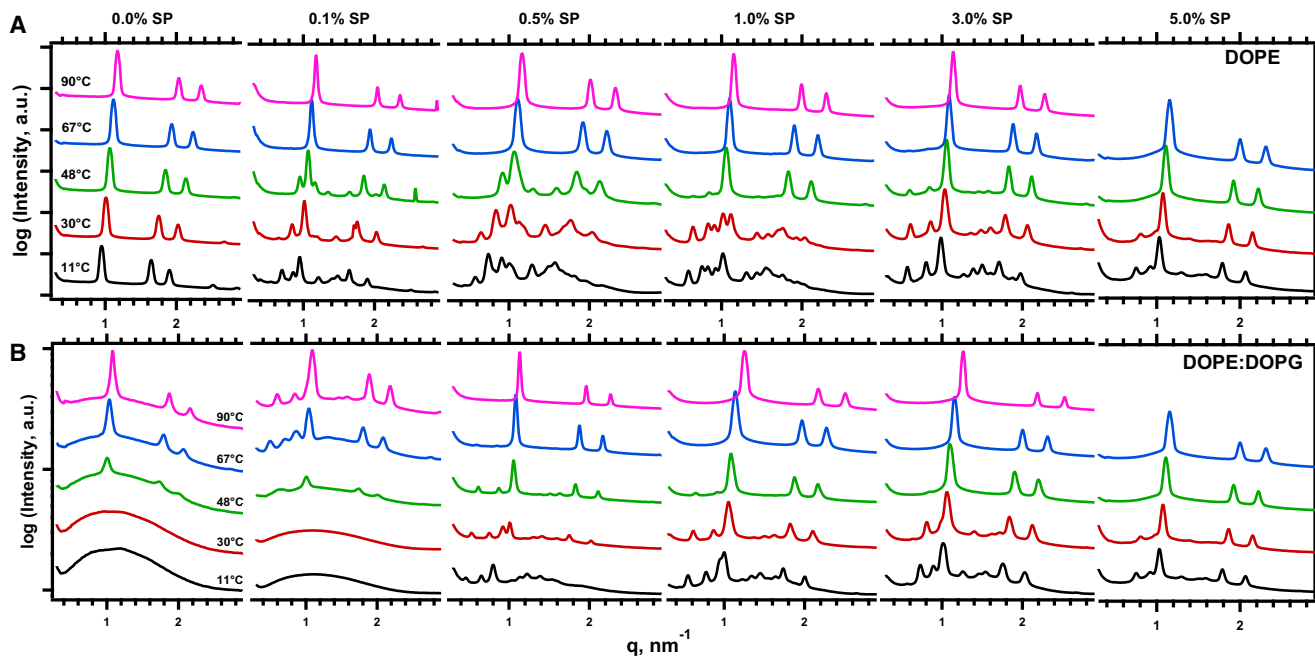
FIGURE 1 Diffraction from phospholipid-protein mixtures. Traces depict radially integrated intensity plotted on a logarithmic scale for a limited range of q. The different sets of data are offset vertically without change in scale to allow inspection of the separated traces. The results show how DOPG, different levels of SP (%, w/w), and temperature affect diffraction from DOPE. Data at additional temperatures and concentrations of protein were omitted for clarity of presentation. Samples contain 2 μM EDTA and 10 mM HEPES, pH 7.0. (*A*) DOPE alone. (*B*) DOPE/DOPG (9:1, mol/mol).

of protein at 0.05% SP, minor peaks with low intensity appeared at intervals that fit with the cubic space groups of the bicontinuous phases. At the lower end of the temperature range, greater amounts of protein initially shifted the relative intensities of cubic and hexagonal diffraction until at 0.5% SP, the Q_{II} phase existed alone (Fig. 1 *A*). In our previous studies with POPE, the Q_{II} phases appeared only above 57°C. With DOPE, the proteins induced their effect at temperatures as low as 11°C. These results eliminated any concerns that the Q_{II} phases observed with POPE might reflect the effects of heat-denatured proteins.

The H_{II} phase was more accessible with DOPE than with POPE. At the lower temperatures, increasing amounts of protein that initially produced more intense cubic diffraction subsequently favored hexagonal structures (Figs. 1 *A* and 2 *A*). Samples at 11°C, for instance, produced only cubic diffraction for 0.25–0.75% SP, but a coexisting hexagonal structure appeared again at 1.0–5.0% SP. Higher temperatures similarly favored the H_{II} phase. The Q_{II} phase that formed at lower temperatures converted during heating to H_{II} structures, without coexisting phases, for the full set of samples with 0–5% SP (Fig. 2 *A*). The samples with DOPE achieved the stated aim of forming hexagonal structures over a broad range of protein concentrations.

The proteins produced a minimal effect on the hexagonal lattice constant ($a_o(H_{II})$) (Figs. 3 *A* and 4 *A*). The response to the proteins depended on temperature. At $\leq$39°C, where coexistence with the Q_{II} phases made the content of SPs in either phase uncertain, greater amounts of protein decreased

$a_o(H_{II})$ (Fig. 4 *A*). At the higher temperatures where the H_{II} phase existed alone, $a_o(H_{II})$ increased with protein by at most a few percent (Fig. 4 *A*). At these temperatures, the $a_o(H_{II})$ for DOPE with 5% SP was indistinguishable from the value for the lipid alone.

Effect of DOPG

Two possibilities could explain the minimal effect of the proteins on $a_o(H_{II})$ for DOPE. The first is related to shape. The curvature of a cylindrical monolayer reflects its composition. The contribution of each component is weighted according to its effective molecular shape (16,36), determined by the relative hydrophobic and hydrophilic cross-sectional areas (18–20). Curvature would be unaffected if the added protein and DOPE have the same molecular shape over the full range of temperatures. The alternative and more likely explanation is that the proteins failed to insert into the H_{II} leaflets.

In addition to the predominant, zwitterionic compounds, ~10% of the phospholipids in pulmonary surfactant are anionic (37,38). The hydrophobic proteins are cationic. Dimeric SP-B has a net charge of +14 (39), and SP-C is +2 or +3, depending on the animal from which it is obtained (40). Electrostatic interactions with anionic phospholipids might allow incorporation of proteins that would otherwise be excluded. We therefore tested whether the addition of 10% DOPG to DOPE would alter the ability of the proteins to change $a_o(H_{II})$.
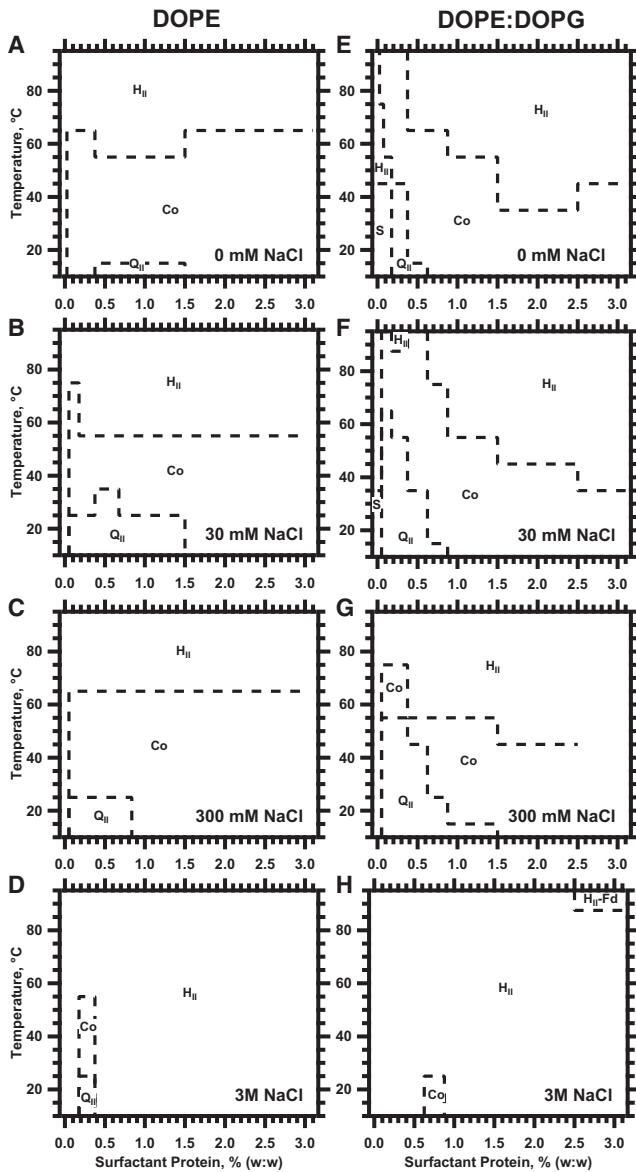
FIGURE 2 Phase diagrams for DOPE (*A–D*) and DOPE/DOPG (9:1, mol/mol) (*E–H*) showing the effects of the hydrophobic proteins and temperature on the phases formed with different concentrations of NaCl. Labels on the graphs indicate regions with the following phases: inverse hexagonal phase (H_{II}); inverse bicontinuous cubic phase without distinction between the Pn$\overline{3}$m and Im$\overline{3}$m space groups (Q_{II}); coexisting H_{II} and Q_{II} phases (*Co*); coexisting H_{II} and Fd$\overline{3}$m phases (H_{II}-*Fd*); and samples that scattered without diffraction (*S*). Diagrams for 100 mM NaCl and 1 M NaCl are omitted for clarity of presentation.

The added anionic phospholipid altered the structures formed by the lipids alone, without the proteins. DOPE/DOPG (9:1, mol/mol) produced only a broad scattering peak at lower temperatures without diffraction (Figs. 1 *B* and 2 *E*). These results were consistent with the disjoining of lipid leaflets caused by electrostatic repulsion, which has prevented measurements of diffraction with charged lipids in previous studies (41,42). Higher temperatures
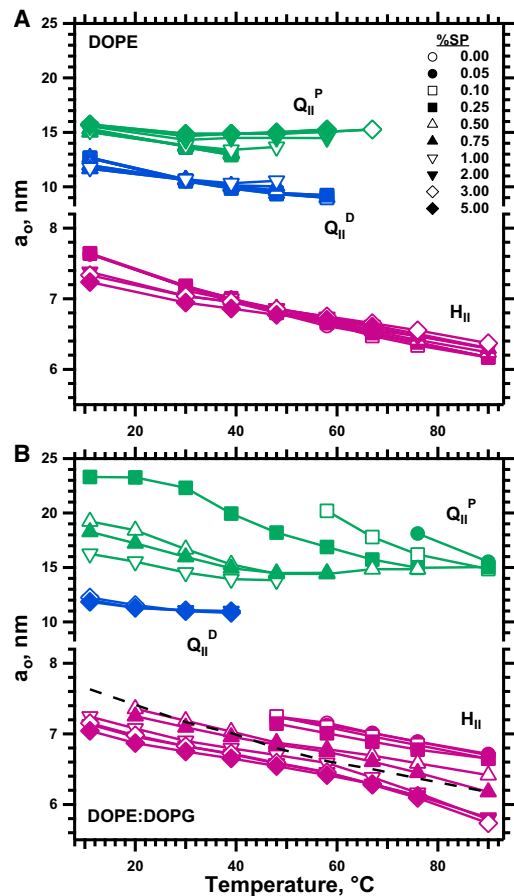

FIGURE 3 Effect of temperature on the lattice constant of structures formed by DOPE and DOPE/DOPG with different amounts of protein. The diffracting structures were identified according to the spacing of the diffraction peaks (Fig. 1) as H_{II} or as Q_{II} with space group either Pn$\overline{3}$m or Im$\overline{3}$m, corresponding to a bicontinuous structure along the diamond (Q_{II}^{D}) or primitive (Q_{II}^{P}) infinitely periodic minimal surface, respectively. The *y* axis is split to emphasize the shift in $a_o(H_{II})$ with different amounts of SP. Samples contained 10 mM HEPES, pH 7.0, and 2 mM EDTA. (*A*) DOPE alone. (*B*) DOPE/DOPG (9:1, mol/mol). The dashed black line indicates the values of $a_o(H_{II})$ for DOPE without DOPG or protein.

produced peaks with hexagonal spacing (Figs. 1 *B* and 2 *E*). Relative to DOPE alone, the added DOPG increased $a_o(H_{II})$ by ~5 Å (Fig. 3 *B*). The anionic lipid by itself, without the proteins, expanded the cylindrical structures for DOPE and decreased the curvature of the lipid leaflet.

The proteins had the opposite effect of decreasing $a_o(H_{II})$ (Figs. 3 *B* and 4 *B*). Scattering and coexistence again complicated analysis of $a_o(H_{II})$ at lower temperatures (Fig. 1 *B*), but above 50°C, the H_{II} phase occurred alone over a broad range of protein concentrations (Fig. 2 *E*). The proteins initially produced a roughly linear decrease in $a_o(H_{II})$ (Fig. 4 *B*). Because the curvature of a cylinder is defined as the reciprocal of its radius (43), $a_o(H_{II})^{-1}$ should track c_o more closely than $a_o(H_{II})$. $a_o(H_{II})^{-1}$ similarly showed an approximately linear variation with added
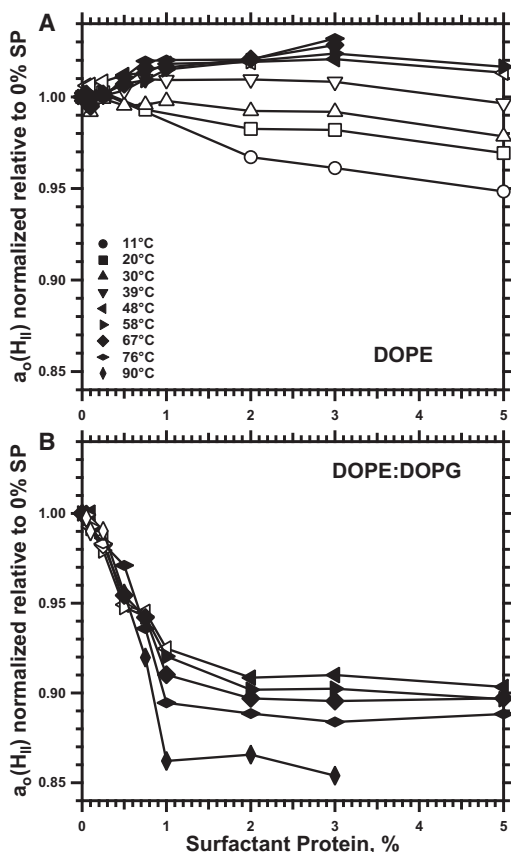
FIGURE 4 Variation of $a_o(H_{II})$ with different concentrations of protein. Traces compare values obtained from Fig. 3 at the same temperature. To correct for the variation of $a_o(H_{II})$ with temperature, values are expressed relative to the value without protein, $a_o/a_o(SP = 0)$. Closed symbols indicate samples with minimal evidence of a coexisting phase; open symbols indicate samples with coexistence. Samples contained 10 mM HEPES, pH 7.0, and 2 mM EDTA. (A) DOPE. (B) DOPE/DOPG (9:1, mol/mol).

protein. Beyond the initial linear variation, however, the effect of the proteins reached an abrupt maximum. More than 1% SP produced minimal additional change in $a_o(H_{II})$ (Fig. 4 B).

Effects of buffered electrolyte

One obvious mechanism by which the proteins might decrease the size of the DOPE/DOPG cylinders was electrostatic. Repulsion among the anionic phospholipids should tend to flatten the curved leaflets and increase $a_o(H_{II})$. Addition of the cationic proteins might decrease these repulsions, allowing the leaflets to approximate more closely the spontaneous curvature that results strictly from their effective molecular shape. Screening by electrolyte in the aqueous medium should minimize electrostatic interactions. We therefore tested whether increasing concentrations of NaCl would alter the effects of the proteins on $a_o(H_{II})$.

For DOPE with the proteins, in both the presence and absence of the anionic lipid, salt changed the phase behavior

(Fig. 2). Higher concentrations of NaCl favored the H_{II} phase. The region in which the Q_{II} phases coexisted with the H_{II} phase narrowed, expanding the range over which the H_{II} phase appeared alone. Higher salt also induced formation of an additional phase. At the highest levels of temperature, protein and salt, along with the hexagonal diffraction, additional peaks appeared at intervals consistent with the $Fd\overline{3}m$ space group (44). Generally, however, the expansion of conditions at which the H_{II} phase occurred alone allowed determination of whether salt affected the influence of the proteins on curvature.

The response of $a_o(H_{II})$ to salt depended on the presence of DOPG and the content of protein. Without the anionic lipid, salt had essentially no effect. $a_o(H_{II})$ for DOPE with all levels of SP changed minimally with increasing concentrations of NaCl (Fig. 5 A). With DOPG present, NaCl produced a small but progressive decrease in $a_o(H_{II})$ with $\leq 0.5\%$ SP (Fig. 5 B). At 3 M NaCl, $a_o(H_{II})$ reverted to the value for DOPE without the DOPG (Fig. 5). With more protein, salt had no effect. Like the samples containing DOPE without DOPG (Fig. 5 A), $a_o(H_{II})$ for DOPE/DOPG with more than 0.5% SP was invariant to the concentration of NaCl (Fig. 5 B).

The liquid layer that lines the alveolus contains calcium as well as NaCl (45). We therefore tested whether the physiological level of 1.5 mM $CaCl_2$ with 150 mM NaCl (HSC) would diminish the effects of the proteins. The $a_o(H_{II})$ for the samples with calcium was essentially unchanged from the values with 100 mM NaCl (Fig. 5, right lower axis). The divalent cation produced no dramatic additional change beyond the effect of the monovalent electrolyte.

Pivotal plane and spontaneous curvature

The change in $a_o(H_{II})$ produced by the proteins (Fig. 4 B) did not necessarily indicate a shift in c_o. Because the curvature of a cylinder is defined as the reciprocal of its radius ($c \equiv 1/R$), the curvature of a monolayer depends on where across the leaflet the radius is measured (Fig. 6). The values of $a_o(H_{II})$ provided the radius at the outer dimension of the cylinder (R_o; Fig. 6). c_o, however, is defined instead at the neutral plane, at which the energies of bending and stretching uncouple, and approximated at the pivotal plane (Fig. 6), where the cross-sectional molecular area remains constant during bending (46). Despite the change in $a_o(H_{II})$ produced by the proteins, c_o might still remain unchanged if the pivotal plane shifted to a sufficiently different location within the lipid leaflet.

An established experimental approach (36,47) determined whether the proteins shifted the pivotal plane within the cylindrical leaflet. This analysis measures the molecular volume, $\Delta\overline{V}_p$, that separates the pivotal plane from the Luzzati surface, which defines the outer edge of the aqueous core (Fig. 6). If the proteins have no effect on $\Delta\overline{V}_p$, then the pivotal plane must remain at a fixed location within
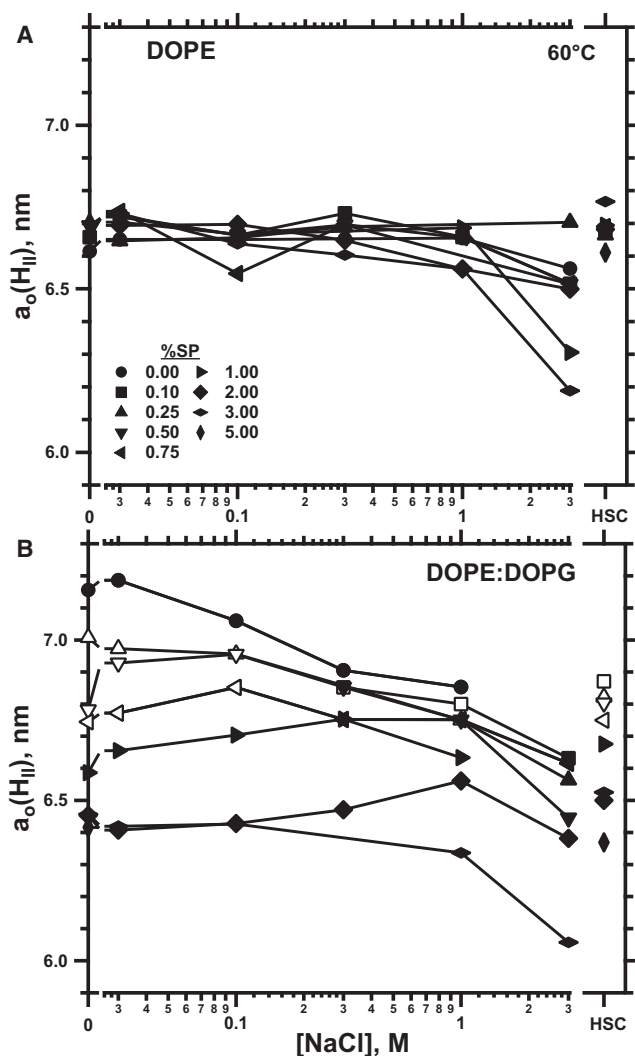
A   DOPE   60°C

%SP
● 0.00   ▶ 1.00
■ 0.10   ◆ 2.00
▲ 0.25   ◆ 3.00
▼ 0.50   ◆ 5.00
◀ 0.75

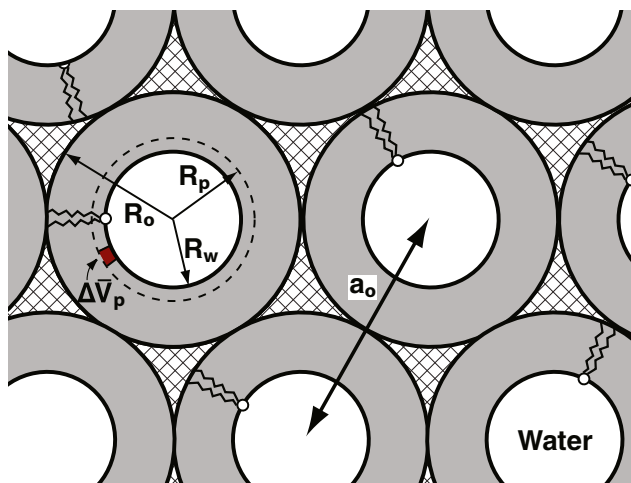B   DOPE:DOPG

[NaCl], M

FIGURE 6 Schematic diagram indicating key features of the H_{II} phase. The gray rings with the sketch of an individual phospholipid represent the cylindrical monolayers surrounding the white aqueous core. The arrows indicate: the lattice constant obtained directly from measurements of diffraction (a_o); the radius at the Luzzati surface at the outer surface of the aqueous core (R_w); the radius at the outer surface of the monolayer (R_o); the radius at the pivotal plane (*dashed ring*), where the molecular cross-sectional area remains constant during bending (R_p); and the molecular volume that separates the pivotal plane from the Luzzati surface ($\Delta\overline{V}_p$). The crosshatched areas represent regions that would be unfilled if the monolayers were circular with a uniform thickness.

FIGURE 5 Response of $a_o(H_{II})$ to variable concentrations of electrolyte. Samples contained lipids combined with different amounts (%, w/w) of proteins and suspended in different concentrations of NaCl buffered with 10 mM HEPES, pH 7.0, at 60°C. HSC samples contained 150 mM NaCl, 1.5 mM $CaCl_2$, and 10 mM HEPES, pH 7.0. Closed symbols indicate measurements that detected only the hexagonal phase; open symbols indicate the presence of coexisting Q_{II} phases. (*A*) DOPE. (*B*) DOPE/DOPG (9:1, mol/mol).

the monolayer. The shift in $a_o(H_{II})$ produced by the proteins would then necessarily reflect a change in c_o. We therefore determined $\Delta\overline{V}_p$ for DOPE/DOPG with three levels of the proteins.

Measurements of $\Delta\overline{V}_p$ required the locations of the pivotal plane and the Luzzati surface. The volume fraction of water in the H_{II} phase, $\phi_w = \overline{V}_w/(\overline{V}_\ell + \overline{V}_w)$, determined the radius at the Luzzati surface (R_w) (46) according to

$$R_W = \sqrt{\frac{\sqrt{3} \times \phi_w}{2\pi}} \times a_o(H_{II}). \qquad (1)$$

Locating the pivotal plane required determination of the molecular area that remained constant during bending. Varying the hydration of the H_{II} phase changed the size of the aqueous core and subjected the leaflet to bending. Analytical expressions provided the molecular area at different radii and established the point at which the area remained unchanged. This analysis provided $\Delta\overline{V}_p$ for each set of samples with a different amount of protein.

The calculations required hexagonal diffraction without coexistence over the full range of hydrations for the samples with all three levels of protein. Measurements performed at temperatures between 10°C and 60°C met that constraint best at 30°C. We therefore restricted our analysis to that temperature.

Changes in hydration produced the expected variation in $a_o(H_{II})$ (Fig. 7). With progressively larger ϕ_w, $a_o(H_{II})$ initially increased, indicating the swelling of the H_{II} cylinders (Fig. 7). $a_o(H_{II})$ then reached a maximum value that remained constant at higher ϕ_w (Fig. 7), indicating that additional water formed a separate aqueous phase without affecting the maximally swollen cylindrical monolayers. The value of ϕ_w at the break in the variation of $a_o(H_{II})$ provided the water content of the fully hydrated H_{II} cylinders. Above the breakpoint, different amounts of protein produced different plateau values of $a_o(H_{II})$ (Fig. 7), indicating a different R_w for the fully hydrated H_{II} phase. The response of $a_o(H_{II})$ in the plateau to increasing amounts of SP replicated the behavior in excess water. $a_o(H_{II})$ dropped
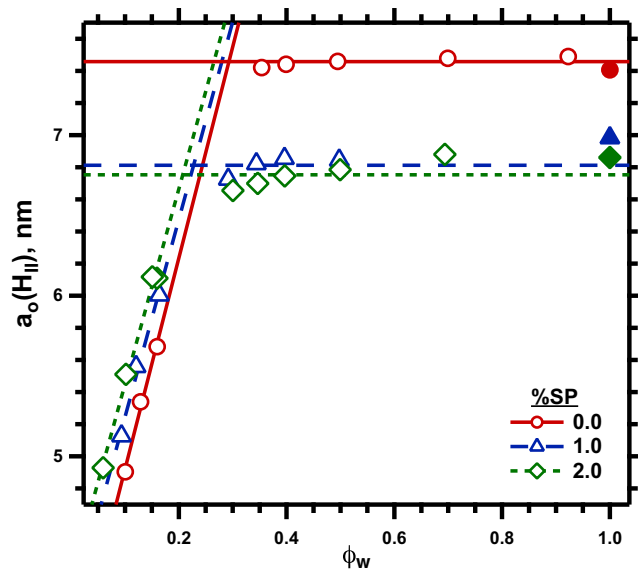
FIGURE 7 Swelling of DOPE/DOPG (9:1, mol/mol) with different amounts of the combined surfactant proteins (%, w/w). Measurements were made at 30°C on samples containing HE added to achieve different levels of hydration. The data were restricted to samples that produced only hexagonal diffraction without evidence for a coexisting phase. The solid symbols indicate results obtained with HE added to excess.

between 0 and 1%SP, but showed little additional change at 2% SP.

The variably swollen H_{II} phase provided the basis for locating the pivotal plane, at which molecular area remained unchanged during bending. The molecular area at the Luzzati surface, $\overline{A}_w$, is given by (46)

$$\overline{A}_w = \frac{2\phi_w \overline{V}_\ell}{(1 - \phi_w)R_w}. \qquad (2)$$

At any other radius, separated from the Luzzati surface by $\Delta\overline{V}_i$, the molecular area, $\overline{A}_i$, would be given by

$$\overline{A}_i^2 = \overline{A}_w^2 + 2\Delta\overline{V}_i \times \frac{\overline{A}_w}{R_w}. \qquad (3)$$

At the pivotal plane, where the molecular area ($\overline{A}_p$) would, by definition, be constant,

$$\overline{A}_w^2 = \overline{A}_p^2 - 2\Delta\overline{V}_p \times \frac{\overline{A}_w}{R_w}. \qquad (4)$$

Plots of $\overline{A}_w^2$ versus $\overline{A}_w/R_w$ fit reasonably well to straight lines (Fig. 8), confirming the existence of a pivotal plane and providing $\Delta\overline{V}_p$ from the slope. For the three levels of protein, the slopes of these plots were indistinguishable (Fig. 8), indicating that the protein had no effect on $\Delta\overline{V}_p$. The invariance of $\Delta\overline{V}_p$ with different amounts of the proteins indicated that they also had no effect on the location of the pivotal plane within the cylindrical monolayer. The shift in $a_o(H_{II})$ produced by the proteins must correspond
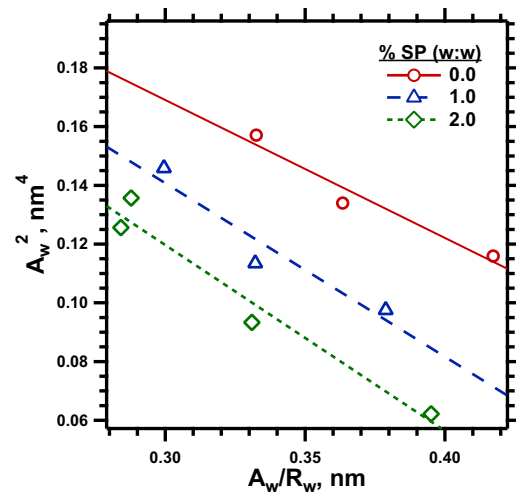
FIGURE 8 Diagnostic plots for samples of DOPE/DOPG with different amounts of the SPs. The data from the ascending limb ($0 < \phi_w < 0.26$) in Fig. 7 were used to calculate values of $\overline{A}_w^2$ and $\overline{A}_w/R_w$. The straight lines represent the least-squares linear fit to the data for each sample.

to a change in the radius at the pivotal plane (R_p). Because $c_o \equiv (R_p)^{-1}$, the proteins therefore also changed the c_o.

The samples with excess water provided values of R_p. A geometric relationship (48) describes the radius, R_i, of any cylindrical surface in terms of its separation, $\Delta\overline{V}_i$, from the Luzzati surface:

$$R_i = R_w \times \left(1 + \frac{1 - \phi_w}{\phi_w} \times \frac{\Delta\overline{V}_i}{\overline{V}_\ell}\right). \qquad (5)$$

With values of $\Delta\overline{V}_p$, this expression provided R_p. The slopes for the samples with the three contents of SP produced an average $\Delta\overline{V}_p = 0.282$ nm³. The breakpoint between the rising limb and the plateau in the swelling plots (Fig. 7) established ϕ_w for the fully hydrated H_{II} cylinders. That value of ϕ_w, together with the average $a_o(H_{II})$ from the plateau, provided an average R_w according to Eq. 1 for the fully hydrated samples with each content of SP. Equation 5 then yielded R_p of 4.1, 4.5, and 4.6 nm for 0%, 1%, and 2% SP, respectively. For the initial 1% change in SP over which the proteins produced a progressive decrease in $a_o(H_{II})$, the c_o changed relative to the lipids alone by 8%.

DISCUSSION

Our results indicate that the hydrophobic SPs can contribute to the negative curvature of lipid leaflets. With appropriate monolayers, the proteins produce a dose-related decrease in $a_o(H_{II})$ and in the cylindrical radius. Because $\Delta\overline{V}_p$ is unaffected by the proteins, the pivotal plane remains at the same location within the monolayer. The smaller a_o produced by the proteins must reflect a more negative c_o.

These findings fit with the prediction that the proteins promote adsorption at least in part by facilitating the

formation by the lipids of curved structures (23,49,50). The model predicts that an intermediate structure between the vesicles and the interfacial film limits the rate of adsorption, and that the proteins promote formation of that structure. The energy required to bend the leaflets from their spontaneous configuration to the structure of the curved intermediate represents one barrier to forming the rate-limiting structure. A change in c_o toward the curvature of the intermediate would reduce that energy of bending. The effect of the proteins on curvature would remain unexpressed in the surfactant lipids except adjacent to the air/water interface, where the reduction in interfacial energy achieved by forming a film would drive formation of the transient, curved intermediate. The demonstration that the proteins can change c_o represents perhaps the most direct evidence yet for the model of the stalk intermediate, and for a mechanism by which the proteins might promote adsorption.

Other mechanisms, of course, remain possible. In terms of the stalk model, the protein could also reduce the energy of bending by changing the bending elasticities (15). The curved intermediate would also involve an unfavorable disruption of chain-packing that the proteins might minimize (16). Our experiments in no way address the relative importance of these other possibilities. Our studies only test and confirm the possibility that the proteins can change c_o.

The effect of the proteins on c_o requires the presence of DOPG. With DOPE alone, the proteins produce no response. The mechanism by which the anionic lipid achieves its effect is uncertain. The most obvious explanation would be strictly electrostatic. Repulsion among the negatively charged DOPG molecules in the monolayer would tend to flatten the leaflet, resulting in the observed enlargement of the H_{II} cylinder. Addition of the positively charged proteins would counteract that repulsion to some extent and allow the leaflet to return to its zwitterionic configuration.

That explanation seems unlikely. Consistent with previously published results (51), screening electrolyte has a limited effect on the expansion caused by DOPG alone. Salt also produced little change in the ability of the proteins to produce a dose-related decrease in $a_o(H_{II})$, or in the magnitude of that effect. Concentrations of salt that reduce the Debye length to ~1 Å produce no shift in the effect of the proteins. These experimental results are consistent with the ratio of charges contributed by the proteins and phospholipids. Previous reports indicate that the physiological mixture contains roughly equal weights of SP-B and SP-C (52–54). At 1% SP, where the proteins reach their maximum effect, the ratio of anionic/cationic charge is ~17 (55). The proteins fall well short of neutralizing the anionic phospholipids. Electrostatic interactions may help the proteins incorporate into the hexagonal lattice, but the contribution of their charge to curvature should be limited.

Interaction between the anionic lipid and the cationic protein could change the effective shape of the proteins and their influence on curvature. Our results suggest, however, that the effect of DOPG may simply reflect a change in the size of the H_{II} cylinder. DOPG enlarges the cylindrical radius above the value for DOPE alone. The proteins produce a dose-related effect on curvature that saturates when the H_{II} cylinders fall to a size slightly below that observed for DOPE alone. These results suggest that DOPG may increase the radii of the cylinders to a value above the minimum required to accommodate the proteins. The effect of the proteins would saturate when the cylindrical radius returns to the minimum size. This possibility is testable. Zwitterionic phospholipids that produce H_{II} cylinders of radius above that minimum should show the effects of the proteins despite their neutral charge. The magnitude of the change produced by the proteins would then depend on the extent to which the cylinder exceeds the minimum size. In a cylindrical monolayer with a bigger radius, the proteins might produce a much larger effect than demonstrated here.

Our samples contained the mixture of SP-B and SP-C isolated together from extracted surfactant. That approach has the advantage that our results reflect the effects of the proteins in their physiological ratio. The disadvantage of our studies is that they provide no insight into the individual roles of SP-B and SP-C. Previous reports suggest that the effects of the combined proteins on both structure and function result mostly from SP-B. That protein has the predominant effect on adsorption (56). Induction of the Q_{II} phases with POPE also results mostly from SP-B (57). The experiments here with the combined proteins, however, leave the effects of the individual proteins on c_o unspecified.

The increased magnitude of curvature induced by the proteins may also explain their effect on compressed films. In the alveolus, after adsorbing to form an interfacial film, the surfactant constituents undergo compression by the shrinking alveolar surface during exhalation. The films avoid collapse and remain at the interface during compression to high densities that reduce surface tension to very low values (23). A monolayer with a greater c_o would presumably have a larger propensity to collapse by folding from the interface. In spread monolayers of the surfactant lipids, the proteins increase the rates of collapse (58), consistent with their effect of increasing curvature. The mechanisms that stabilize the alveolar films remain unknown, but they may involve a compositional change. Bronchoalveolar lavage recovers the surfactant lipids in roughly equal amounts as large aggregates that contain the proteins and resemble the lamellar bodies secreted by type II pneumocytes, and as small vesicles that lack the proteins (59–61). Exposure to a cycling air/water interface converts the large aggregates to the smaller forms (62–64). These results suggest that in the alveolus, the proteins at some point separate from the surfactant lipids. That separation, and the elimination of the effect on curvature, may be crucial for the ability of surfactant films to reach low surface tension.

In summary, in the presence of 10% DOPG, the hydrophobic surfactant proteins induce DOPE to adopt more

negative spontaneous curvature. These results are consistent with the model in which the proteins promote adsorption by facilitating formation of a negatively curved structure that limits the rate of adsorption to the air/water interface.

REFERENCES

1. Lachmann, B., G. Grossmann, …, B. Robertson. 1979. Lung mechanics during spontaneous ventilation in premature and fullterm rabbit neonates. *Respir. Physiol.* 38:283–302.

2. Clements, J. A. 1977. Functions of the alveolar lining. *Am. Rev. Respir. Dis.* 115(6 II):67–71.

3. Sen, A., S.-W. Hui, …, E. A. Egan. 1988. Localization of lipid exchange sites between bulk lung surfactants and surface monolayer: freeze fracture study. *J. Colloid Interface Sci.* 126:355–360.

4. Schürch, S., D. Schürch, …, B. Robertson. 1994. Surface activity of lipid extract surfactant in relation to film area compression and collapse. *J. Appl. Physiol.* 77:974–986.

5. Haller, T., P. Dietl, …, G. Putz. 2004. Tracing surfactant transformation from cellular release to insertion into an air-liquid interface. *Am. J. Physiol. Lung Cell. Mol. Physiol.* 286:L1009–L1015.

6. Chernomordik, L., A. Chanturiya, …, J. Zimmerberg. 1995. The hemifusion intermediate and its conversion to complete fusion: regulation by membrane composition. *Biophys. J.* 69:922–929.

7. Yu, S.-H., P. G. R. Harding, and F. Possmayer. 1984. Artificial pulmonary surfactant. Potential role for hexagonal H_{II} phase in the formation of a surface-active monolayer. *Biochim. Biophys. Acta.* 776:37–47.

8. Perkins, W. R., R. B. Dause, …, A. S. Janoff. 1996. Role of lipid polymorphism in pulmonary surfactant. *Science.* 273:330–332.

9. Biswas, S. C., S. B. Rananavare, and S. B. Hall. 2005. Effects of gramicidin-A on the adsorption of phospholipids to the air-water interface. *Biochim. Biophys. Acta.* 1717:41–49.

10. Loney, R. W., W. R. Anyan, …, S. B. Hall. 2011. The accelerated late adsorption of pulmonary surfactant. *Langmuir.* 27:4857–4866.

11. Fuller, N., and R. P. Rand. 2001. The influence of lysolipids on the spontaneous curvature and bending elasticity of phospholipid membranes. *Biophys. J.* 81:243–254.

12. Biswas, S. C., S. B. Rananavare, and S. B. Hall. 2007. Differential effects of lysophosphatidylcholine on the adsorption of phospholipids to an air/water interface. *Biophys. J.* 92:493–501.

13. Whitsett, J. A., W. M. Hull, …, T. E. Weaver. 1986. Immunologic identification of a pulmonary surfactant-associated protein of molecular weight = 6000 daltons. *Pediatr. Res.* 20:744–749.

14. Reference deleted in proof.

15. Helfrich, W. 1973. Elastic properties of lipid bilayers: theory and possible experiments. *Z. Naturforsch. C.* 28:693–703.

16. Gruner, S. M. 1989. Stability of lyotropic phases with curved interfaces. *J. Phys. Chem.* 93:7562–7570.

17. Kahn, M. C., G. J. Anderson, …, S. B. Hall. 1995. Phosphatidylcholine molecular species of calf lung surfactant. *Am. J. Physiol.* 269:L567–L573.

18. Israelachvili, J. N., S. Marcelja, and R. G. Horn. 1980. Physical principles of membrane organization. *Q. Rev. Biophys.* 13:121–200.

19. Tanford, C. 1973. The Hydrophobic Effect: Formation of Micelles and Biological Membranes. Wiley, New York.

20. Tartar, H. V. 1955. A theory of the structure of the micelles of normal paraffin-chain salts in aqueous solution. *J. Phys. Chem.* 59:1195–1199.

21. Tate, M. W., and S. M. Gruner. 1987. Lipid polymorphism of mixtures of dioleoylphosphatidylethanolamine and saturated and monounsaturated phosphatidylcholines of various chain lengths. *Biochemistry.* 26:231–236.

22. Rand, R. P., N. L. Fuller, …, V. A. Parsegian. 1990. Membrane curvature, lipid segregation, and structural transitions for phospholipids under dual-solvent stress. *Biochemistry.* 29:76–87.

23. Rugonyi, S., S. C. Biswas, and S. B. Hall. 2008. The biophysical function of pulmonary surfactant. *Respir. Physiol. Neurobiol.* 163:244–255.

24. Chavarha, M., H. Khoojinian, …, S. B. Hall. 2010. Hydrophobic surfactant proteins induce a phosphatidylethanolamine to form cubic phases. *Biophys. J.* 98:1549–1557.

25. Gruner, S. M. 1989. Hydrocarbon chain conformation in the H_{II} phase. *Biophys. J.* 56:1045–1049.

26. Shyamsunder, E., S. M. Gruner, …, C. P. Tilcock. 1988. Observation of inverted cubic phase in hydrated dioleoylphosphatidylethanolamine membranes. *Biochemistry.* 27:2332–2336.

27. Hall, S. B., Z. Wang, and R. H. Notter. 1994. Separation of subfractions of the hydrophobic components of calf lung surfactant. *J. Lipid Res.* 35:1386–1394.

28. Takahashi, A., and T. Fujiwara. 1986. Proteolipid in bovine lung surfactant: its role in surfactant function. *Biochem. Biophys. Res. Commun.* 135:527–532.

29. Curstedt, T., H. Jörnvall, …, P. Berggren. 1987. Two hydrophobic low-molecular-mass protein fractions of pulmonary surfactant. Characterization and biophysical activity. *Eur. J. Biochem.* 168:255–262.

30. Taneva, S. G., J. Stewart, …, K. M. Keough. 1998. Method of purification affects some interfacial properties of pulmonary surfactant proteins B and C and their mixtures with dipalmitoylphosphatidylcholine. *Biochim. Biophys. Acta.* 1370:138–150.

31. Kaplan, R. S., and P. L. Pedersen. 1985. Determination of microgram quantities of protein in the presence of milligram levels of lipid with amido black 10B. *Anal. Biochem.* 150:97–104.

32. Ames, B. N. 1966. Assay of inorganic phosphate, total phosphate and phosphatases. *Methods Enzymol.* 8:115–118.

33. Hammersley, A. P., S. O. Svensson, …, D. Hausermann. 1996. Two-dimensional detector software: From real detector to idealised image or two-theta scan. *High Press. Res.* 14:235–248.

34. Sun, R. G., and J. Zhang. 2004. The cubic phase of phosphatidylethanolamine film by small angle x-ray scattering. *J. Phys. D Appl. Phys.* 37:463–467.

35. Ladbrooke, B. D., R. M. Williams, and D. Chapman. 1968. Studies on lecithin-cholesterol-water interactions by differential scanning calorimetry and x-ray diffraction. *Biochim. Biophys. Acta.* 150:333–340.

36. Gruner, S. M. 1985. Intrinsic curvature hypothesis for biomembrane lipid composition: a role for nonbilayer lipids. *Proc. Natl. Acad. Sci. USA.* 82:3665–3669.

37. Pfleger, R. C., and H. G. Thomas. 1971. Beagle dog pulmonary surfactant lipids. Lipid composition of pulmonary tissue, exfoliated lining cells and surfactant. *Arch. Intern. Med.* 127:863–872.

38. Pfleger, R. C., R. F. Henderson, and J. Waide. 1972. Phosphatidyl glycerol—a major component of pulmonary surfactant. *Chem. Phys. Lipids.* 9:51–68.

39. Johansson, J., T. Curstedt, and H. Jörnvall. 1991. Surfactant protein B: disulfide bridges, structural properties, and kringle similarities. *Biochemistry.* 30:6917–6921.

40. Haagsman, H. P., and R. V. Diemel. 2001. Surfactant-associated proteins: functions and structural variation. *Comp. Biochem. Physiol. A Mol. Integr. Physiol.* 129:91–108.

41. Hauser, H. 1984. Some aspects of the phase behaviour of charged lipids. *Biochim. Biophys. Acta.* 772:37–50.

42. Gulik-Krzywicki, T., A. Tardieu, and V. Luzzati. 1969. The smectic phase of lipid-water systems: properties related to the nature of the lipid and to the presence of net electrical charges. *Mol. Cryst. Liq. Cryst.* 8:285–291.

43. Hyde, S. 1997. The Language of Shape. The Role of Curvature in Condensed Matter: Physics, Chemistry, and Biology. Elsevier, Amsterdam, New York.

44. Seddon, J. M., J. Robins, …, H. Delacroix. 2000. Inverse micellar phases of phospholipids and glycolipids. *Phys. Chem. Chem. Phys.* 2:4485–4493.

45. Nielson, D. W. 1986. Electrolyte composition of pulmonary alveolar subphase in anesthetized rabbits. *J. Appl. Physiol.* 60:972–979.

46. Kozlov, M. M. 2007. Determination of lipid spontaneous curvature from X-ray examinations of inverted hexagonal phases. *Methods Mol. Biol.* 400:355–366.

47. Kooijman, E. E., V. Chupin, …, P. R. Rand. 2005. Spontaneous curvature of phosphatidic acid and lysophosphatidic acid. *Biochemistry.* 44:2097–2102.

48. Leikin, S., M. M. Kozlov, …, R. P. Rand. 1996. Measured effects of diacylglycerol on structural and elastic properties of phospholipid membranes. *Biophys. J.* 71:2623–2632.

49. Walters, R. W., R. R. Jenq, and S. B. Hall. 2000. Distinct steps in the adsorption of pulmonary surfactant to an air-liquid interface. *Biophys. J.* 78:257–266.

50. Klenz, U., M. Saleem, …, H. J. Galla. 2008. Influence of lipid saturation grade and headgroup charge: a refined lung surfactant adsorption model. *Biophys. J.* 95:699–709.

51. Alley, S. H., O. Ces, …, R. H. Templer. 2008. X-ray diffraction measurement of the monolayer spontaneous curvature of dioleoylphosphatidylglycerol. *Chem. Phys. Lipids.* 154:64–67.

52. Pérez-Gil, J., A. Cruz, and C. Casals. 1993. Solubility of hydrophobic surfactant proteins in organic solvent/water mixtures. Structural studies on SP-B and SP-C in aqueous organic solvents and lipids. *Biochim. Biophys. Acta.* 1168:261–270.

53. van Eijk, M., C. G. De Haas, and H. P. Haagsman. 1995. Quantitative analysis of pulmonary surfactant proteins B and C. *Anal. Biochem.* 232:231–237.

54. Baatz, J. E., Y. Zou, …, R. H. Notter. 2001. High-yield purification of lung surfactant proteins sp-b and sp-c and the effects on surface activity. *Protein Expr. Purif.* 23:180–190.

55. Schram, V., W. R. Anyan, and S. B. Hall. 2003. Non-cooperative effects of lung surfactant proteins on early adsorption to an air/water interface. *Biochim. Biophys. Acta.* 1616:165–173.

56. Wang, Z., O. Gurel, …, R. H. Notter. 1996. Differential activity and lack of synergy of lung surfactant proteins SP-B and SP-C in interactions with phospholipids. *J. Lipid Res.* 37:1749–1760.

57. Chavarha, M., R. W. Loney, …, S. B. Hall. 2012. Differential effects of the hydrophobic surfactant proteins on the formation of inverse bicontinuous cubic phases. *Langmuir.* 28:16596–16604.

58. Lhert, F., W. Yan, …, S. B. Hall. 2007. Effects of hydrophobic surfactant proteins on collapse of pulmonary surfactant monolayers. *Biophys. J.* 93:4237–4243.

59. Wright, J. R., B. J. Benson, …, J. A. Clements. 1984. Protein composition of rabbit alveolar surfactant subfractions. *Biochim. Biophys. Acta.* 791:320–332.

60. Lewis, J. F., M. Ikegami, and A. H. Jobe. 1990. Altered surfactant function and metabolism in rabbits with acute lung injury. *J. Appl. Physiol.* 69:2303–2310.

61. Hall, S. B., R. W. Hyde, and R. H. Notter. 1994. Changes in subphase aggregates in rabbits injured by free fatty acid. *Am. J. Respir. Crit. Care Med.* 149:1099–1106.

62. Gross, N. J., and K. R. Narine. 1989. Surfactant subtypes of mice: metabolic relationships and conversion in vitro. *J. Appl. Physiol.* 67:414–421.

63. Gross, N. J., and K. R. Narine. 1989. Surfactant subtypes in mice: characterization and quantitation. *J. Appl. Physiol.* 66:342–349.

64. Hall, S. B., R. W. Hyde, and M. C. Kahn. 1997. Stabilization of lung surfactant particles against conversion by a cycling interface. *Am. J. Physiol.* 272:L335–L343.